REFERENCES

[1] W. D. Squire, H. J. Whitehouse, and J. M. Alsup, "Linear signal processing and ultrasonic transversal filters," *IEEE Trans. Microwave Theory Tech.* (*Special Issue on Microwave Acoustics*), vol. MTT-17, pp. 1020–1040, Nov. 1969.
[2] R. H. Tancrell and M. G. Holland, "Acoustic surface wave filters," *Proc. IEEE*, vol. 59, pp. 393–409, Mar. 1971.
[3] M. Waldner, M. E. Pedinoff, and H. M. Gerard, "Broadband surface wave nonlinear convolution filters," in *Proc. 1971 IEEE Symp. Ultrasonics* (Miami Beach, Fla.), Dec. 6–8, 1971.
[4] R. L. Zimmerman, B. P. Schweitzer, and R. C. Bender, "High data rate-high bit density acoustic digital memory," in *Proc. 1972 IEEE Symp. Ultrasonics* (Boston, Mass.), Oct. 4–7, 1972, pp. 459–364.
[5] W. R. Smith, H. M. Gerard, and W. R. Jones. "Analysis and design of dispersive interdigital surface-wave transducers," *IEEE Trans. Microwave Theory Tech.*, vol. MTT-20, pp. 458–471, July 1972.
[6] W. R. Smith, H. M. Gerard, J. H. Collins, T. M. Reeder, and H. J. Shaw, "Analysis of interdigital surface wave transducers by use of an equivalent circuit model," *IEEE Trans. Microwave Theory Tech.* (*Special Issue on Microwave Acoustics*), vol. MTT-17, pp. 856–864, Nov. 1969.
[7] Coquin and Tiesten, *J. Acoust. Soc. Amer.*, vol. 41, Apr. 1967.
[8] G. R. Nudd, "Technique for varying the conversion loss against frequency of a surface wave transducer without apodization," *Electron. Lett.*, vol. 8, July 1972.
[9] M. Waldner, "Application of nonlinear interactions in acoustic media to microwave signal processing devices," Rome Air Development Center, Rome, N.Y., Contract F30602-71-C-0196, Final Rep., Aug. 1972.
[10] M. Golay, "Complementary series," *IRE Trans. Inform. Theory*, vol. IT-7, pp. 82–87, Apr. 1961.
[11] B. P. Schweitzer and J. M. Speiser, "Generalized complementary code sets," in *Proc. IEEE Int. Symp. Information Theory* (Pacific Grove, Calif.), Jan. 31–Feb. 3, 1972, p. 102.
[12] A. Papoulis, *The Fourier Integral and Its Application.* New York: McGraw-Hill, 1962, ch. 7.
[13] R. B. Rice, "Inverse convolution filters," *Geophys.*, vol. 27, pp. 4–18, Feb. 1962.
[14] R. D. Weglein and G. R. Nudd, "Space-harmonic response of surface wave transducers," in *Proc. 1972 IEEE Symp. Ultrasonics* (Boston, Mass.), Oct. 4–7, 1972, pp. 346–352.
[15] M. T. Wauk and R. L. Zimmerman, "Bonded planar structures for efficient surface wave generation," in *Proc. 1972 IEEE Symp. Ultrasonics* (Boston, Mass.), Oct. 4–7, pp. 365–366.
[16] R. C. Williamson and H. I. Smith, "Large time bandwidth product surface wave pulse compressor employing reflective gratings," *Electron. Lett.*, vol. 8, 1972.

High-Permittivity Dielectrics in Waveguides and Resonators

JEAN VAN BLADEL, SENIOR MEMBER, IEEE

***Abstract*—Resonators and waveguides containing a region of high dielectric constant are considered. The dielectric constant is first assumed to be infinite, but is later given a high, but finite value. Perturbation formulas are derived for the resulting shift in either the resonant frequency of the resonator or the wavenumber of the waveguide mode.**

I. INTRODUCTION

MATERIALS of high dielectric constant and low loss-factor are now available to the microwave community. Typical values of the dielectric constant are 10 for alumina substrates, 33–38 for temperature-stable ceramics containing zirconates, and 100 or more for materials such as rutile or strontium titanate [1], [2]. Consider a cavity containing a dielectric of high dielectric constant ϵ_r and a given resonant mode therein, the lowest for example (Fig. 1). The resonant wavelength is of the order of the typical dimensions L and L_d of the cavity. Now let ϵ_r increase without limit. The resonant wavelength in the dielectric remains of the order of L_d, while the resonant frequency approaches zero. Expressed more quantitatively: a) λ_{diel} approaches a value αL_d, where α is a coefficient of order one; b) the wavenumber in the dielectric approaches a limit $k = 2\pi/\lambda_{\text{diel}} = 2\pi/\alpha L_d$; and c) the wavenumber *in vacuo* approaches a value $k/n = (1/n)(2\pi/\alpha L_d)$. Here, $n = (\epsilon_r)^{1/2}$ is the index of refraction of the dielectric. It is seen that the resonant frequency, given by $\omega/c = k/n$, approaches a value

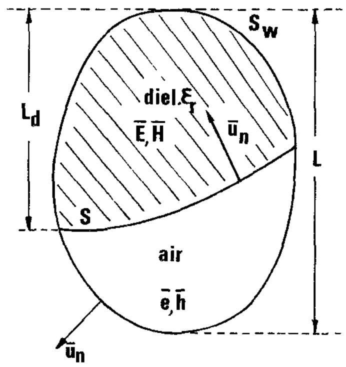

Fig. 1. Resonant cavity containing a dielectric.

$$f = \frac{c}{n\alpha L_d} = \frac{1}{2\pi}\frac{c}{n}k. \tag{1}$$

It is the purpose of this paper to calculate a second-order correction term for (1), i.e., to obtain the first two terms in a series

$$f = \frac{A}{n} + \frac{B}{n^2} + \cdots. \tag{2}$$

Manuscript received February 5, 1973; revised July 31, 1973.
The author is with the Laboratory for Electromagnetism and Acoustics, University of Ghent, Ghent, Belgium.

With such an expression, better values of the resonant frequency can be obtained. The method implies that the series converges fast, i.e., that its first two terms are a good representation of its value. In practice, the dielectric sample must be large enough, given the value of ϵ_r. If the sample is too small, the dielectric "loses control," and perturbational techniques of the "small-sample" type should be used [3]. When applicable, the method represents a substantial saving in computation time when a broad range of values of ϵ_r is under consideration, e.g., when the influence of small fluctuations in the value of ϵ_r is investigated.

II. General Formulas for the Resonant Cavity

The resonant electric eigenvectors in a cavity containing a medium of variable dielectric constant ϵ_r satisfy the equations [4]

$$\frac{1}{\epsilon_r}\,\text{curl curl}\,\boldsymbol{E} = \gamma^2 \boldsymbol{E}$$

$$\boldsymbol{u}_n \times \boldsymbol{E} = 0, \qquad \text{on the metallic walls } S_w. \tag{3}$$

The $\boldsymbol{E}$ vectors are real. Their associated magnetic eigenvectors are of the form $1/\nu$ curl $\boldsymbol{E}$. In the configuration of Fig. 1, the dielectric consists of air and a region of dielectric constant $\epsilon_r = n^2$. We shall use capital letters for the fields in the dielectric and lower case letters for the fields in the air region. With this notation, (3) becomes

$$-\text{curl curl}\,\boldsymbol{E} + k^2\boldsymbol{E} = 0$$

$$-\text{curl curl}\,\boldsymbol{e} + \frac{k^2}{n^2}\boldsymbol{e} = 0. \tag{4}$$

Equation (4) is complemented by boundary conditions on the perfectly conducting walls S_w and by the requirement that the tangential components of the electric field and its curl be continuous across the S interface. For high values of ϵ_r, the fields approach limits satisfying

$$-\text{curl curl}\,\boldsymbol{E}_0 + k_0^2\boldsymbol{E}_0 = 0$$

$$\begin{cases} -\text{curl curl}\,\boldsymbol{e}_0 = 0 \\ \text{div}\,\boldsymbol{e}_0 = 0. \end{cases} \tag{5}$$

The subscript 0 refers to the asymptotic condition $n = \infty$. For n high, but not infinite, the fields and wavenumbers take the form $\boldsymbol{E} = \boldsymbol{E}_0 + \boldsymbol{E}_1$, $\boldsymbol{e} = \boldsymbol{e}_0 + \boldsymbol{e}_1$, $k = k_0 + k_1$, where the terms with subscript 1 are perturbation terms. Insertion in (3) yields, for small perturbational corrections,

$$-\text{curl curl}\,\boldsymbol{E}_1 + k_0^2\boldsymbol{E}_1 = -2k_0k_1\boldsymbol{E}_0$$

$$\begin{cases} -\text{curl curl}\,\boldsymbol{e}_1 = -\dfrac{k_0^2}{n^2}\boldsymbol{e}_0 \\ \text{div}\,\boldsymbol{e}_1 = 0. \end{cases} \tag{6}$$

Equation (6) is complemented by the boundary conditions mentioned above, which hold for the 0 and 1 fields separately. Notice that the "tangential" conditions on S also imply satisfaction of the "normal" conditions

$$\boldsymbol{u}_n\cdot\boldsymbol{E}_0 = 0$$

$$\boldsymbol{u}_n\cdot\boldsymbol{E}_1 = \frac{1}{n^2}(\boldsymbol{u}_n\cdot\boldsymbol{e}_0). \tag{7}$$

In order to solve (6), it is necessary to know k_1, the shift in wavenumber due to the finite character of ϵ_r. This quantity can be calculated directly from $\boldsymbol{E}_0$ and $\boldsymbol{e}_0$, without explicit solution of (6). The calculation is effected by applying a well-known Green's theorem to the air region:

$$\iiint_{\text{air}} [-\boldsymbol{e}_1\cdot\text{curl curl}\,\boldsymbol{e}_0 + \boldsymbol{e}_0\cdot\text{curl curl}\,\boldsymbol{e}_1]\,dV$$

$$= \iint_S [(\boldsymbol{u}_n\times\boldsymbol{e}_1)\cdot\text{curl}\,\boldsymbol{e}_0 - (\boldsymbol{u}_n\times\boldsymbol{e}_0)\cdot\text{curl}\,\boldsymbol{e}_1]\,dS$$

$$= \frac{k_0^2}{n^2}\iiint_{\text{air}} (\boldsymbol{e}_0)^2\,dV \tag{8}$$

where use has been made of (6). Similarly, the dielectric region yields

$$\iiint_{\text{diel}} [-\boldsymbol{E}_1\cdot\text{curl curl}\,\boldsymbol{E}_0 + \boldsymbol{E}_0\cdot\text{curl curl}\,\boldsymbol{E}_1]\,dV$$

$$= \iint_S [-(\boldsymbol{u}_n\times\boldsymbol{E}_1)\cdot\text{curl}\,\boldsymbol{E}_0 - (\boldsymbol{u}_n\times\boldsymbol{E}_0)\cdot\text{curl}\,\boldsymbol{E}_1]\,dS$$

$$= 2k_0k_1\iiint_{\text{diel}} (\boldsymbol{E}_0)^2\,dV. \tag{9}$$

Adding (8) and (9) together causes the surface integrals to cancel because of the boundary conditions along S. There remains

$$k_1 = -\frac{k_0}{2n^2}\left(\iiint_{\text{air}} (\boldsymbol{e}_0)^2\,dV \Big/ \iiint_{\text{diel}} (\boldsymbol{E}_0)^2\,dV\right). \tag{10}$$

This is the desired relationship for the shift in k, which is seen to be proportional to $1/\epsilon_r = 1/n^2$. Having found k_1, it is now possible to solve for $\boldsymbol{e}_1$ and $\boldsymbol{E}_1$ from (6). Both perturbation fields are evidently proportional to $1/\epsilon_r$.

III. Verification on a Particular Resonator Mode

As an example of application, we consider one of the modes of the cavity depicted in Fig. 2. The modes can be obtained by separation of variables. Our choice falls on

$$e_x = \frac{\pi}{d}\cos\frac{\pi x}{d}\sin u\frac{y+l}{l}\sin\frac{\pi z}{h}$$

$$e_y = -\frac{l}{u}\left[\left(\frac{\pi}{d}\right)^2 + \left(\frac{\pi}{h}\right)^2\right]\sin\frac{\pi x}{d}\cos u\frac{y+l}{l}\sin\frac{\pi z}{h}$$

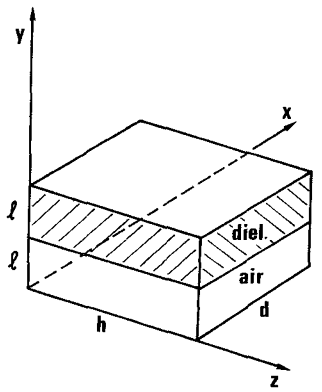

Fig. 2. Resonant cavity in the form of a parallelepiped.

$$e_z = \frac{\pi}{h} \sin \frac{\pi x}{d} \sin u \frac{y+l}{l} \cos \frac{\pi z}{h}$$

$$E_x = -\frac{\pi}{d} \frac{\sin u}{\sin v} \cos \frac{\pi x}{d} \sin v \frac{y-l}{l} \sin \frac{\pi z}{h}$$

$$E_y = \frac{l}{v} \frac{\sin u}{\sin v} \left[\left(\frac{\pi}{d}\right)^2 + \left(\frac{\pi}{h}\right)^2 \right] \sin \frac{\pi x}{d} \cos v \frac{y-l}{l} \sin \frac{\pi z}{h}$$

$$E_z = -\frac{\pi}{h} \frac{\sin u}{\sin v} \sin \frac{\pi x}{d} \sin v \frac{y-l}{l} \cos \frac{\pi z}{h} \qquad (11)$$

where

$$u = \left(\frac{k^2}{n^2} - \frac{\pi^2}{d^2} - \frac{\pi^2}{h^2}\right)^{1/2} l \quad \text{and} \quad v = \left(k^2 - \frac{\pi^2}{d^2} - \frac{\pi^2}{h^2}\right)^{1/2} l.$$

The resonant wavenumbers for arbitrary n are given by the transcendental equation

$$n^2 u \operatorname{tg} u + v \operatorname{tg} v = 0. \qquad (12)$$

We have solved this equation for the geometrical parameters $d = 1.7l$ and $h = 2.6l$. The (exact) results are given in Table I. The quantities of interest are the dimensionless parameters kl and $\nu l = kl/n = \omega l/c$; where νl is proportional to the resonant frequency. Notice that this frequency decreases for increasing ϵ_r, as mentioned in Section I. The results denoted as pert. (for perturbation) are obtained from (10). Application of this formula requires knowledge of the $\boldsymbol{E}_0$ and $\boldsymbol{e}_0$ fields, which can easily be derived from (11) by setting $v = \pi/2$ and $u = (k^2 l^2 - \pi^2/4)^{1/2}$ [see (11) and (12)].

TABLE I
RESONANT WAVENUMBERS FOR A CAVITY

$n^2 = \epsilon_r$	kl(exact)	kl(pert.)	νl(exact)	νl(pert.)
2.25	2.5053	2.5220	1.6702	1,6813
4	2.5987	2.6048	1.2993	1,3024
9	2.6617	2.6628	0,8872	0,8876
16	2.6829	2.6833	0,6707	0,6708
∞	2.7097	2.7097	0	0

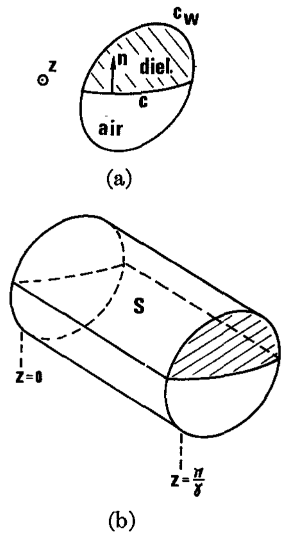

Fig. 3. (a) Cross section of a waveguide containing a dielectric. (b) Resonant cavity derived from the waveguide.

The first two terms in the expansion for kl are

$$kl = 2.7097 - \frac{0.4225}{n^2}. \qquad (13)$$

It is seen from Table I that exact and perturbed values are in excellent agreement for $n^2 = 16$, and are still not too far apart for $n^2 = 2.25$.

IV. General Formulas for Waveguides

In each region of the waveguide shown in Fig. 3(a), the modal components are of the form [4]

$$E_z(xyz) = A_z(xy) e^{j\gamma z}$$

$$H_z(xyz) = B_z(xy) e^{j\gamma z}$$

$$\boldsymbol{E}_{tr}(xyz) = \frac{1}{\kappa^2 - \gamma^2} \left(j\gamma \operatorname{grad} A_z - j\omega\mu \boldsymbol{u}_z \times \operatorname{grad} B_z \right) e^{j\gamma z}$$

$$= \boldsymbol{A}_t(xy) e^{j\gamma z}$$

$$\boldsymbol{H}_{tr}(xyz) = \frac{1}{\kappa^2 - \gamma^2} \left(j\gamma \operatorname{grad} B_z - j\omega\epsilon \boldsymbol{u}_z \times \operatorname{grad} A_z \right) e^{j\gamma z}$$

$$= \boldsymbol{B}_t(xyz) e^{j\gamma z} \qquad (14)$$

where κ is the wavenumber relative to the region. We shall reserve the notation A_i, B_i ($i = x,y,z$) for the components in the dielectric, and denote the analogous components in air by a_i, b_i. The various components satisfy

$$\nabla_{xy}^2 A_i + (k^2 - \gamma^2) A_i = 0, \quad \text{in the dielectric}$$

$$\nabla_{xy}^2 a_i + \left(\frac{k^2}{n^2} - \gamma^2\right) a_i = 0, \quad \text{in air.} \qquad (15)$$

These equations are complemented by the usual boundary condition on the tangential components of A and B along boundary curve c, and by the boundary conditions on the metallic boundary C_W, i.e., $A_z = \partial B_z / \partial n = 0$.

Consider first the modal components for $n^2 = \infty$. They satisfy

$$\nabla_{xy}^2 A_i + (k^2 - \gamma^2) A_i = 0, \quad \text{in the dielectric}$$
$$\nabla_{xy}^2 a_{0i} - \gamma^2 a_{0i} = 0, \quad \text{in air.} \qquad (16)$$

When ϵ_r is finite, these components are modified by perturbational terms A_{1i} and a_{1i}, which are seen, by substitution in (15), to satisfy

$$\nabla_{xy}^2 A_{1i} + (k^2 - \gamma^2) A_{1i} = -2k_0 k_1 A_{0i}$$
$$\nabla_{xy}^2 a_{1i} - \gamma^2 a_{1i} = -\frac{k_0^2}{n^2} a_{0i}. \qquad (17)$$

In deriving these equations, we have assumed that γ, the propagation constant, is held constant. To solve (17), it is necessary to obtain an expression for k_1, the shift in wavenumber k. Here, as usual, a Green's theorem must be introduced. The simplest method is perhaps to start with the superposition of a wave of type (14) and a similar wave with $e^{-j\gamma z}$ as a phase factor. This gives a total field of the form

$$\boldsymbol{E} = A_z \cos \gamma z \boldsymbol{u}_z + j \sin \gamma z \boldsymbol{A}_t. \qquad (18)$$

Expressions of this kind can be written for the 0 fields and the 1 fields separately. In both cases, $\boldsymbol{E}$ can be interpreted as a resonant field for the volume bounded by the waveguide wall and the metallized end planes $z = 0$ and $z = \pi/\gamma$ [Fig. 3(b)]. The $\boldsymbol{E}$ field given in (18) has zero divergence, so that $-\text{curl curl } \boldsymbol{E}$ can be replaced by $\nabla^2 \boldsymbol{E}$. We shall now apply the vector Green's theorem

$$\iiint [-\boldsymbol{a} \cdot \text{curl curl } \boldsymbol{b} + \boldsymbol{b} \cdot \text{curl curl } \boldsymbol{a}] \, dV$$
$$= \iint_S [(\boldsymbol{u}_n \times \boldsymbol{a}) \cdot \text{curl } \boldsymbol{b} - (\boldsymbol{u}_n \times \boldsymbol{b}) \cdot \text{curl } \boldsymbol{a}] \, dS \qquad (19)$$

to the air volume in Fig. 3(b), having set $\boldsymbol{a} = \boldsymbol{e}_0$ and $\boldsymbol{b} = \boldsymbol{e}_1$. Because $\nabla^2 \boldsymbol{e}_0 = 0$ and $\nabla^2 \boldsymbol{e}_1 = -(k_0^2/n^2) \boldsymbol{e}_0$, this gives

$$\iiint_{\text{air}} (\boldsymbol{e}_0 \cdot \nabla^2 \boldsymbol{e}_1 - \boldsymbol{e}_1 \cdot \nabla^2 \boldsymbol{e}_0) \, dV$$
$$= -\frac{k_0^2}{n^2} \iiint_{\text{air}} \boldsymbol{e}_0 \cdot \boldsymbol{e}_0 \, dV$$
$$= -\frac{k_0^2}{n^2} \iiint_{\text{air}} [a_{0z}^2 \cos^2 \gamma z + (j\boldsymbol{a}_{0t}) \cdot (j\boldsymbol{a}_{0t}) \sin^2 \gamma z] \, dV$$
$$= -\frac{k_0^2}{n^2} \frac{\pi}{2\gamma} \iint [a_{0z}^2 + (j\boldsymbol{a}_{0t})^2] \, dS$$
$$= \iint_S [(\boldsymbol{u}_n \times \boldsymbol{e}_0) \cdot \text{curl } \boldsymbol{e}_1 - (\boldsymbol{u}_n \times \boldsymbol{e}_1) \cdot \text{curl } \boldsymbol{e}_0] \, dS. \qquad (20)$$

Similarly, in the dielectric region, where $\nabla^2 \boldsymbol{E}_0 = -k_0^2 \boldsymbol{E}_0$ and $\nabla^2 \boldsymbol{E}_1 = -k_0^2 \boldsymbol{E}_1 - 2k_0 k_1 \boldsymbol{E}_0$,

$$\iiint_{\text{diel}} [\boldsymbol{E}_0 \cdot \nabla^2 \boldsymbol{E}_1 - \boldsymbol{E}_1 \cdot \nabla^2 \boldsymbol{E}_0] \, dV$$
$$= -2k_0 k_1 \frac{\pi}{2\gamma} \iint [A_{0z}^2 + (j\boldsymbol{A}_{0t})^2] \, dS$$
$$= -\iint_S [(\boldsymbol{u}_n \times \boldsymbol{E}_0) \cdot \text{curl } \boldsymbol{E}_1 - (\boldsymbol{u}_n \times \boldsymbol{E}_1) \cdot \text{curl } \boldsymbol{E}_0] \, dS. \qquad (21)$$

Adding (20) and (21) together causes the surface integrals to cancel out because of the boundary conditions on S. There remains

$$k_1 = -\frac{k_0}{2n^2} \cdot \left(\iint_{\text{air}} [a_{0z}^2 + (j\boldsymbol{a}_{0t})^2] \, dS \Big/ \iint_{\text{diel}} [A_{0z}^2 + (j\boldsymbol{A}_{0t})^2] \, dS \right). \qquad (22)$$

This is our fundamental formula. By use of (22), the dispersion curve for arbitrary values of $\epsilon_r = n^2$ can be obtained by starting from the curve for $n^2 = \infty$, drawn once and for all. From a point A of this curve, we set out a length $AB = k_1 = \alpha/n^2$, where the value of α can be calculated from (22). Point B is now a point of the curve $n^2 \neq \infty$. The accuracy of the so-obtained dispersion curve increases with increasing n^2. Calculation of α is the main problem. It must be effected for each point A, and it is therefore interesting to obtain, without increase of labor, a second point of 2 for each A. This is possible by noticing that curves 1 and 2 are locally parallel for high values of n^2. Therefore (Fig. 4)

$$AC = AB \left(\frac{d\gamma}{dk} \right)_A = \alpha \left(\frac{d\gamma}{dk} \right)_A \frac{1}{n^2}. \qquad (23)$$

The formula breaks down at cutoff ($\gamma = 0$, point M), where the tangent is vertical. In the vicinity of M, curve 1 can be approximated by a parabola:

$$k - k_M = \beta \gamma^2.$$

For high values of n^2, curve 2 is almost parallel with 1,

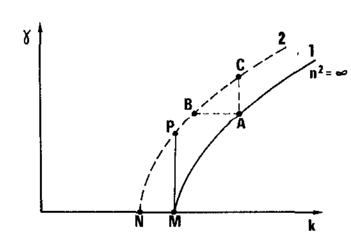

Fig. 4. Obtaining the dispersion curve for $n^2 \neq \infty$ from the curve for $n^2 = \infty$.

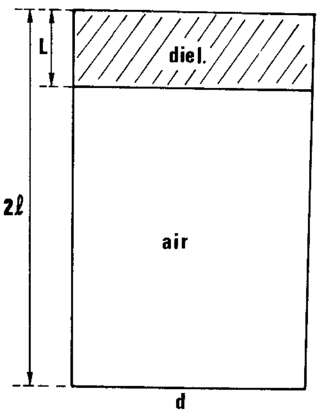

Fig. 5. Cross section of a rectangular waveguide.

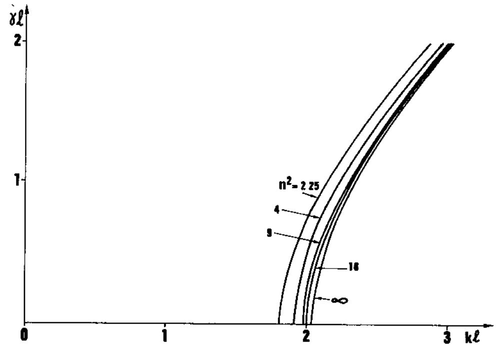

Fig. 6. Exact dispersion curves for the $m = 0$ mode of a rectangular waveguide half filled with dielectric.

TABLE II
WAVENUMBER k FOR 50-PERCENT DIELECTRIC FILLING ($L = l$)

	mode m = 0 (γl = 0)		mode m = 1 (γl = 0)		mode m = 0 (γl = 1)	
n^2	(kl)exact	(kl)pert.	(kl)exact	(kl)pert.	(kl)exact	(kl)pert.
2.25	1.8165	1.8264	0.9331	0.5542	2.1397	2.1642
4	1.9106	1.9150	1.1677	1.0542	2.2360	2.2447
9	1.9772	1.9782	1.4352	1.4532	2.3003	2.3019
16	1.9999	1.9999	1.5724	1.5857	2.3216	2.3220
∞	2.0288	2.0288	1.7562	1.7562	2.3480	2.3480

TABLE III
WAVENUMBER kl FOR THE $m = 0$ MODE

	20% filling (L=0.4l)				10% filling (L=0.2l)			
	γl = 0		γl = 1		γl = 0		γl = 1	
n^2	(kl) exact	(kl) pert.	(kl) exact	(kl) pert.	(kl) exact	(kl) pert.	(kl) exact	(kl) pert.
9	3.6167	3.7146	4.0986	4.1938				
25	4.0652	4.0821	4.4573	4.4702	6.7302	7.2526	7.5442	7.8682
36	4.1369	4.1453	4.5116	4.5178	7.2729	7.5398	7.9266	8.0713
100	4.2360	4.2371	4.5861	4.5869	7.9265	7.9576	8.3509	8.3666
400					8.1320	8.1338	8.4903	8.4912
∞	4.2888	4.2888	4.6258	4.6258	8.1925	8.1925	8.5328	8.5328

and we write $MN = \beta PM^2$, which implies that

$$PM = \left(\frac{\alpha}{\beta}\right)^{1/2} \frac{1}{n} = \left(\frac{MN}{\beta}\right)^{1/2}.$$

The ordinate in M is therefore proportional to $1/n$, and is bound to be a worse approximation than the lengths MN, AB, and AC, all of which are proportional to $1/n^2$.

V. VERIFICATION ON THE MODES OF A RECTANGULAR WAVEGUIDE

The modes of a rectangular waveguide with dielectric slab (Fig. 5) can be obtained by separation of variables [5]. The solutions are shown in Fig. 6. For small values of $d/2l$, the lowest mode is a TE mode with components independent of x (the $m = 0$ mode). For higher values of $d/2l$, the lowest mode has components proportional with $\sin \pi x/d$ or $\cos \pi x/d$ (the $m = 1$ mode). We shall not write down the field components and dispersion relationships explicitly, but will only quote numerical results. Consider first a guide half filled with dielectric ($L = l$) and compare the exact cutoff values (point N in Fig. 4) with the perturbed values, given, respectively, by $kl = 2.0288 [1 - (0.2243/n^2)]$ for the $m = 0$ mode, and $kl = 1.7562 [1 - (1.5532/n^2)]$ for the $m = 1$ mode, value computed for $d = 4l$. Values of the cutoff wavenumber appear in Table II under the heading $\gamma l = 0$.

It is seen that the agreement is excellent for the $m = 0$ mode, but is somewhat worse for the $m = 1$ mode. This is reflected by the first-order correction terms which are, respectively, $0.2243/n^2$ and $1.5532/n^2$. It is to be expected that smaller correction terms give better accuracy, as the second-order terms should be of the order of the square of the first-order ones. We have also given the value of kl for a typical point A of the dispersion curve (point $\gamma l = 1$).

The excellent agreement obtained for 50-percent dielectric filling deteriorates, as expected, when the height of the dielectric slab decreases. This is apparent from a comparison of the results of Tables II and III. At 10-percent filling, the results of $n^2 = 25$ are some 8 percent off in absolute value at cutoff, but the error on k_1/k, the relative frequency shift, is higher and reaches 50 percent. Clearly, the method breaks down completely for lower values of n^2 and is therefore unsatisfactory for handling the modes of, for example, the microstrip in a box configuration (where the filling coefficient is typically 10 percent). The higher modes of the microstrip are very similar to those of the waveguide of Fig. 5 and should therefore behave in a similar manner for high values of ϵ_r [6].

ACKNOWLEDGMENT

The author wishes to thank P. Lootens for his calculations.

REFERENCES

[1] A. Okaya and L. F. Barash, "The dielectric microwave resonator," *Proc. IRE*, vol. 50, pp. 2081–2092, Oct. 1962.
[2] A. Fox, "Temperature-stable low-loss microwave filters using

dielectric resonators," *Electron. Lett.*, vol. 8, pp. 582–583, Nov. 16, 1972.
[3] R. A. Waldron, *The Theory of Waveguides and Cavities*. London, England: Maclaren, 1967.
[4] J. Van Bladel, *Electromagnetic Fields*. New York: McGraw-Hill, 1964, pp. 323–324, 447–450.
[5] J. Van Bladel and T. J. Higgins, "Cut-off frequency in two-dielectric layered rectangular waveguides," *J. Appl. Phys.*, vol. 22, pp. 329–334, Mar. 1951.
[6] G. Essayag and B. Sauve, "Study of higher-order modes in a microstrip structure," *Electron. Lett.*, vol. 8, pp. 564–566, Nov. 16, 1972.

Noise Considerations in Self-Mixing IMPATT-Diode Oscillators for Short-Range Doppler Radar Applications

MADHU-SUDAN GUPTA, MEMBER, IEEE, RONALD J. LOMAX, SENIOR MEMBER, IEEE, AND GEORGE I. HADDAD, FELLOW, IEEE

Abstract—**The influence of the oscillator noise on the minimum detectable signal of a Doppler radar with a self-mixing IMPATT-diode oscillator is evaluated. For very short-range radars, it is the AM noise which limits the signal-to-noise ratio and thus the range.**

I. Introduction

THE PURPOSE of this paper is to investigate the influence of oscillator noise on the performance of a self-mixing CW short-range Doppler radar in order to determine the oscillator noise requirements for a given application, or alternatively, to find the minimum detectable signal for a given oscillator. The effect of the AM, FM, and video noise of a self-mixing IMPATT-diode oscillator used in a short-range radar on the signal-to-noise ratio and the minimum detectable signal will be evaluated, and a simple expression for the amplitude of the detected Doppler signal will be given. The effect of $1/f$ noise is not included in this analysis and is not considered to be appreciable for a well-designed silicon IMPATT oscillator.

IMPATT diodes are particularly attractive mixers for two reasons. First, they can generate oscillations and can be used as "self-pumped" frequency converters, thus eliminating the need for a separate oscillator [1]. Second, they are negative conductance nonlinear devices and therefore offer the possibility of a large conversion gain [2]. IMPATT diodes have been used as self-oscillating frequency converters in two different modes: that in which the signal is uncorrelated to the "local oscillator" output [1] (the usual mixer application) and that in which the signal is derived from the local oscillator output [3], [4] (as in Doppler radars). While the noisiness of the former is adequately described by the noise figure of the mixer, perhaps a more appropriate characterization of noise performance in the second case is the signal-to-noise ratio or the minimum detectable signal for the oscillator-mixer combination.

CW Doppler radars may be classified as long-range radars and short-range ones. To be specific, a short-range radar is one in which the two-way transit time τ_t of the signal between the antenna and the target is very small compared to the period $1/f_d$ of the Doppler shift frequency. Long-range radars have received the most attention in the literature and the influence of oscillator noise on radar performance has been studied by Raven [5] and others. The present study differs from these earlier studies in two important respects: the oscillator and mixer are not separate units and the radar range is smaller (of the order

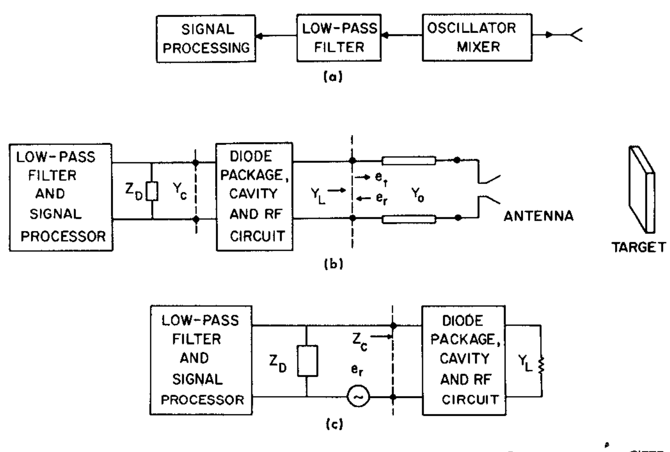

Fig. 1. Schematic diagram and models for a short-range CW Doppler radar with a self-mixing oscillator. (a) Radar system with a self-mixing oscillator. (b) Load-variation-detector model. (c) Injected-signal model.

Manuscript received February 12, 1973; revised May 24, 1973. This work was supported by the U.S. Army Electronics Command under Contract DAAB07-71-C-0244.

M.-S. Gupta is with the Department of Electrical Engineering, Massachusetts Institute of Technology, Cambridge, Mass. 02139.
R. J. Lomax and G. I. Haddad are with the Electron Physics Laboratory, Department of Electrical and Computer Engineering, University of Michigan, Ann Arbor, Mich. 48104.